SAE TECHNICAL PAPER SERIES

2004-01-1584

Fuzzy Logic-Based Smart Battery State-of-Charge (SOC) Monitor for Automotive Batteries

Chakradhar Pulamarasetty and Pritpal Singh
Villanova University

Huiming Chen, Xiquan Wang and David Reisner
US Nanocorp®,Inc.

Wsewolod Hnatczuk
US Army, TACOM.

ISBN 0 7680 1423-9

9 780768 014235

SAE International™

2004 SAE World Congress
Detroit, Michigan
March 8-11, 2004

400 Commonwealth Drive, Warrendale, PA 15096-0001 U.S.A. Tel: (724) 776-4841 Fax: (724) 776-5760 Web: www.sae.org

For permission and licensing requests contact:

SAE Permissions
400 Commonwealth Drive
Warrendale, PA 15096-0001-USA
Email: permissions@sae.org
Fax: 724-772-4891
Tel: 724-772-4028

For multiple print copies contact:

SAE Customer Service
Tel: 877-606-7323 (inside USA and Canada)
Tel: 724-776-4970 (outside USA)
Fax: 724-776-1615
Email: CustomerService@sae.org

ISBN 0-7680-1319-4

Printed in USA

2004-01-1584

Fuzzy Logic-Based Smart Battery State-of-Charge (SOC) Monitor for Automotive Batteries

Chakradhar Pulamarasetty and Pritpal Singh
Villanova University

Huiming Chen, Xiquan Wang and David Reisner
US Nanocorp®,Inc.

Wsewolod Hnatczuk
US Army, TACOM.

ABSTRACT

Automotive start, light, ignition (SLI) lead acid batteries used in tanks are prone to capacity loss due to low temperatures, self-discharge, sulfation and shorting of plates. Monitoring and charge control of these batteries can be improved by using the concept of a smart battery system (SBS). In a SBS, battery data from sensors embedded in the battery package are acquired by a smart battery controller which processes this data, and transmits charge control information, to a central processor for effecting control actions over a controller area network (CAN) bus.

Smart battery circuitry has been designed, developed and implemented to monitor the SOC of a 12V automotive lead acid battery used in tanks. The hardware comprises ac impedance measuring hardware interfaced to a Motorola 68HC12 microcontroller with a built-in CAN controller interface. The SOC estimation algorithms are based on a fuzzy logic model that is directly implemented into the Motorola 68HC12 microcontroller. Details of the hardware and fuzzy logic model design will be presented.

INTRODUCTION

Monitoring SOC is crucial for improving the life and performance of SLI lead acid batteries. Since 1997, Villanova University and US Nanocorp, Inc. have collaborated on the development of patented fuzzy logic-based methods for determining SOC and state-of-health (SOH) of a battery [1,2]. In order to implement the fuzzy logic algorithm for battery SOC determination, many special calculations are required and memory space is required to store both the fuzzy logic model itself and the results of intermediate calculations. We previously presented the design of a custom-designed SOC monitor chip that efficiently performs the fuzzy logic calculations used in our approach to SOC determination [3]. In the previous version of our design, battery temperature, voltage and current were the inputs used to estimate the battery's SOC based on a coulomb counting method. However, a more accurate approach for SOC estimation employs ac impedance measurements and has the added advantage of being able to provide information on the battery's SOH [4].

The circuit design required to accomplish this task involves using analog circuitry for the impedance magnitude measurement and a mixed signal circuit design for phase detection. The custom microcontroller optimized for implementing fuzzy logic algorithms whose structure was described at the 40th Power Sources Conference is then interfaced to the ac impedance measuring circuitry to estimate the battery SOC. In this paper, we present the design of the AC impedance measuring circuitry together with the fuzzy logic model for SOC estimation along with test results for the sub-circuits. Furthermore, we describe a second-generation design that employs a commercial microcontroller, the Motorola 68HC12. This particular microcontroller offers several useful features including fuzzy logic instructions built into the chip's instruction set and a CAN network interface that can be used to enhance the performance of the smart battery controller while concomitantly reducing the size of the board.

AC IMPEDANCE MEASUREMENT CIRCUITRY

In order to measure the impedance of the battery, an AC signal current must be injected into the battery under test as shown in Fig. 1. A four-terminal measurement is used to eliminate contact resistance effects. Usually i_{ac} and v_{ac} are too small to be measured directly, and hence some amplification stages must be provided to amplify these signals as shown in Fig. 2. Following the gain stages, rectifiers and low pass filters can be used to obtain a DC output signal, which will be proportional to the amplitude of the battery impedance. A phase detector is also used to measure the phase angle of the output signal relative to the input signal. Details of this circuit are presented later in the paper. A block diagram of the complete system is shown in Fig. 3.

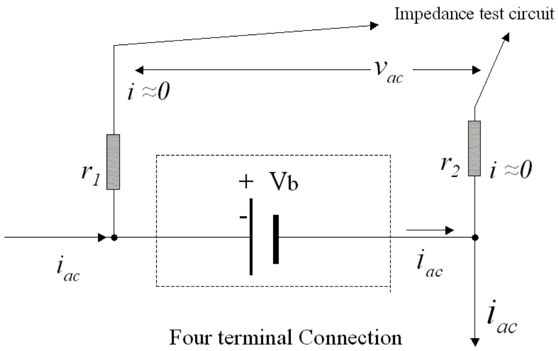

$$Z = V_{ac}/i_{ac} \quad \text{or} \quad |Z| = \frac{|V_{ac}|}{|i_{ac}|}, \quad \theta = \angle(V_{ac}) - \angle(i_{ac})$$

Figure 1 Injection of current source for battery

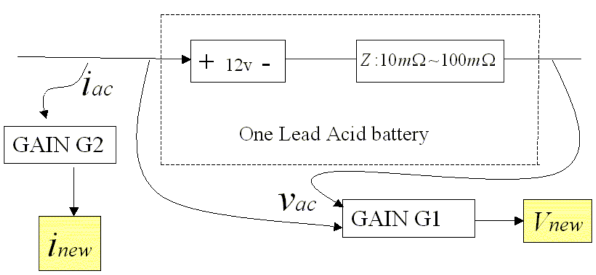

Figure 2 Amplification of small signals

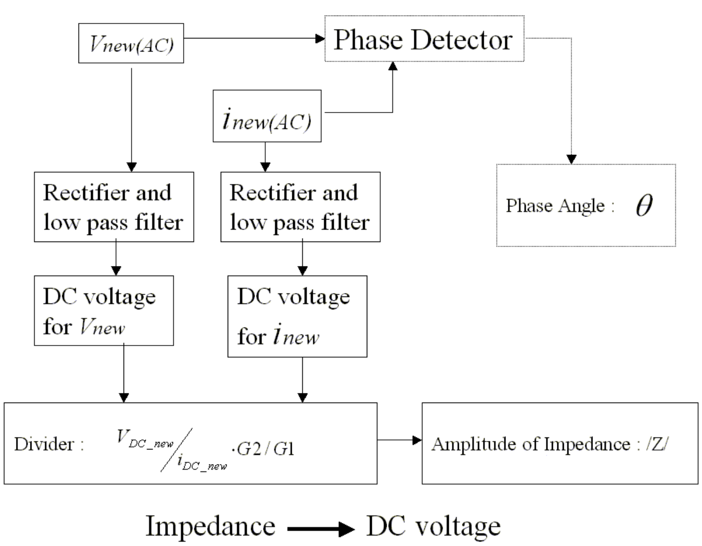

Figure 3 Rectifier and filter for AC-to-DC conversion

In order to reduce circuit power consumption, we developed an improved AC current source, shown in Fig. 4. In Fig. 4, a large value capacitor is used to isolate the DC voltage between the power supply and the tested battery so that the voltage of the power supply does not need to be higher than that of the tested battery. The feedback from the output is used to ensure that the average voltage of the output is equal to half the value of the power supply so that the maximum non-distorted AC value can be obtained at the output (a measured output waveform is shown in Fig. 4.) The feedback from the batt_n node is used to ensure that the current through the tested battery will follow the signal of AC_input. This circuit consumes about 50% less power than conventional AC current sources.

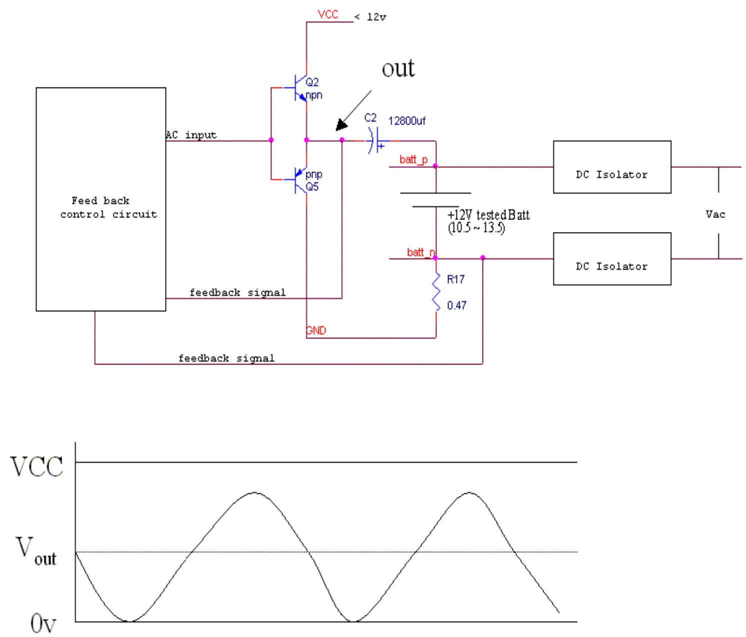

Figure 4 Improved AC current source

The amplitude of the AC test current should be above 300mA, and the actual required value will depend on the internal impedance of the battery under test. If small alkaline cells are used to provide the power for this circuit, they will discharge very quickly and will therefore not provide a practical solution. In order to solve this problem, we have designed a power supply whose power comes from the battery under test. This power supply, shown in Fig. 5, can provide +/-5v the voltage requirement for our current source and other circuits. In this circuit, isolated DC to DC converters are just like a load for the battery under test, and the only effect of these two converters is that some current *i* will go through the battery under test. If the filter can work well, the extra current *i* will be a DC value or at least it will be almost a DC value, and then its effect on the AC voltage of the tested battery can be easily filtered by DC isolator.

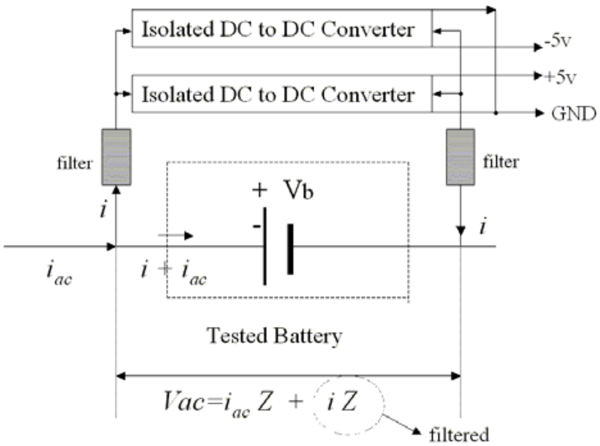

Figure 5 Improved power supply for +/-5V.

AC IMPEDANCE PHASE ANGLE MEASUREMENT CIRCUIT DESIGN

The main function of the phase detector, shown in Fig. 6, is to detect the phase difference between two sinusoidal signals with the same frequency. AC1 and AC2 are two sinusoidal signals and their average value is zero. The waveforms for this detector are shown in Fig. 7. From Fig. 7, it is easy to conclude that the phase angle should be as follows:

If $\theta 1 > \theta 2$, then AC1 leads AC2 by a phase angle $\theta 1$.

If $\theta 2 > \theta 1$, then AC2 leads AC1 by a phase angle $\theta 2$.

($-180^0 < \theta 1, \theta 2 < +180^0$).

Therefore, by measuring the DC voltages of $\theta 1$ and $\theta 2$, the phase difference between the two signals AC1 and AC2 can be easily calculated. This phase detector has passed the test on the breadboard level. The IC design for this detector has also been completed, and the chip fabricated. Testing of this chip has also been successfully completed.

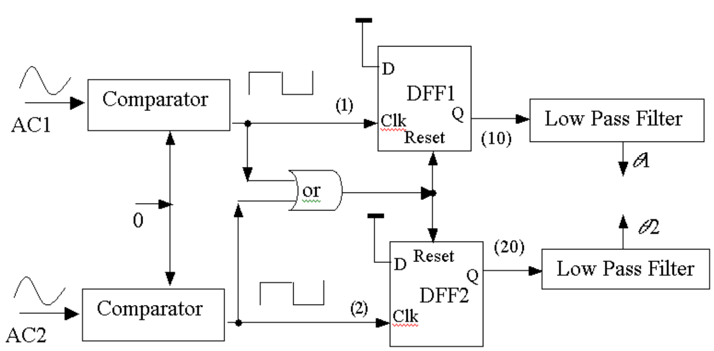

Figure 6 Phase Detector Diagram

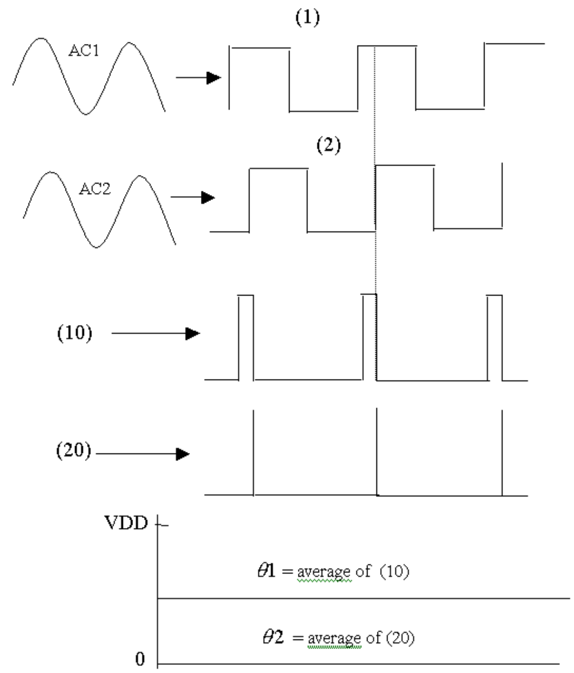

Figure 7 Sample Waveforms for Phase Detector

PRINTED CIRCUIT BOARD LAYOUT

The devices have been implemented at the breadboard level and in printed circuit boards. Fig. 8 shows a photograph of the board populated with the components for the complete board that would be implemented in the battery casing.

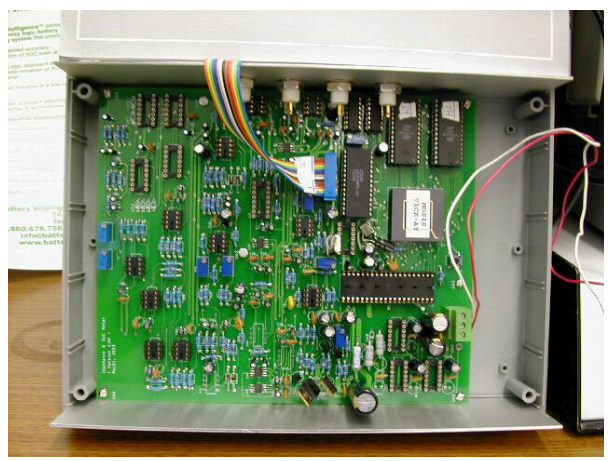

Figure 8 Photograph of Printed Circuit Board of Smart Battery Controller

AC IMPEDANCE CIRCUIT TEST RESULTS

All the circuits have been successfully tested except the improved power supply, which is still undergoing testing. The rest of the ac impedance measurement circuits were tested by making magnitude and phase angle measurements at three different test frequencies (10 Hz, 100Hz and 1 kHz) on an Exide US6TMF and comparing the results with a commercial instrument (Solartron 1280B Electrochemical Measurement Unit). An external +/-5V power supply was used to power our circuitry for this testing. Test results are shown in Table 1 and clearly show good agreement with measurements made with our

Frequency	Impedance (our circuit) |Z|/phase angle *mΩ / degree*	Impedance (Solartron 1280B) |Z|/phase angle *mΩ / degree*
10Hz	14.8 / -0.6	14.6 / -0.5
100Hz	12.6 / 0.1	12.5 / 0.1
1000Hz	15.3 / 1.1	15.1 / 1.0

Table 1 Test results for AC Impedance Measurement Circuit

test circuitry and measurements made with the Solartron unit. However, compared to the Solartron unit, our circuit is much smaller, consumes much less power and may be implemented in the smart battery application (of course it is not as versatile or as capable as the Solartron instrument.)

AC IMPEDANCE MEASUREMENTS ON AUTOMOTIVE BATTERIES

Galvanostatic ac impedance measurements were made on 12V Exide US6TMF 100Ah batteries under open circuit conditions using a Solartron 1280B Electrochemical Measurement Unit. The measurements were made at an AC signal amplitude of 500 mA over the frequency range of 1Hz to 10kHz. Measurements were made at four different temperatures (-20°C, 0°C, 20°C, and 40°C) on three different batteries. The test procedure was as follows:
1) Charge battery
2) Discharge battery at constant current of 1.5A for 30 mins.
3) Rest at open circuit for 1 min.
4) Measure ac impedance
5) Repeat steps 2-4 until a cutoff voltage of 10.2V was reached.
Some sample test data is shown in Fig. 9. It can be clearly seen from Fig. 9 that there is a monotonic change in both the magnitude of the ac impedance at frequencies less than approx. 500Hz and phase angles less than 40Hz. Good discrimination is seen in both the magnitude and phase angle data at 10Hz and a preliminary fuzzy logic model to estimate battery SOC at different temperatures has been developed simply based on this data. This model and its performance is described next.

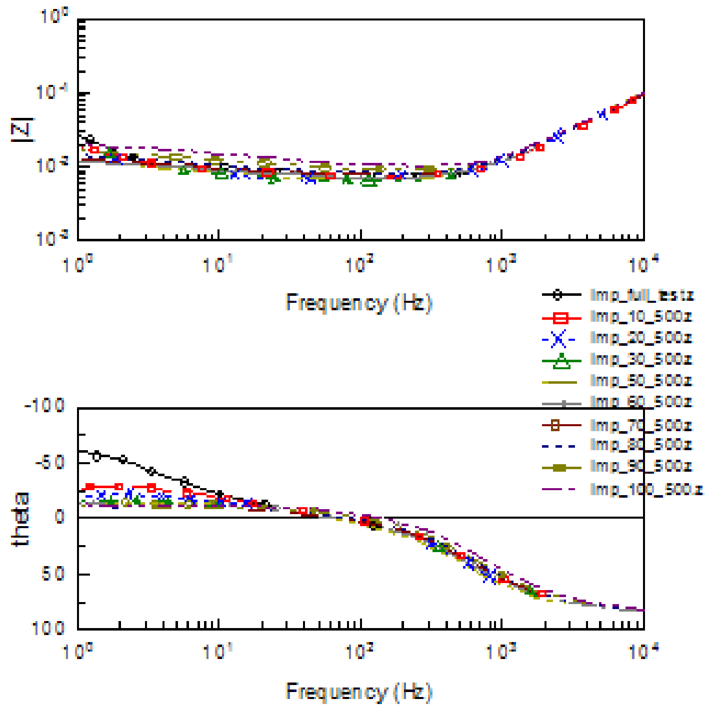

Figure 9. Magnitude and Phase Angle Bode Plots for an Exide US6TMF Battery at different depths of discharge measured at a temperature of 0°C

FUZZY LOGIC MODEL FOR BATTERY SOC ESTIMATION

A preliminary fuzzy logic model has been developed for estimating the SOC of the Exide US6TMF batteries over the temperature range of -20°C to 40°C simply using the impedance magnitude and phase angle at 10Hz of the battery and the battery's temperature as the model inputs. The fuzzy logic model was developed using the Fuzzy Logic Toolbox for Matlab [5]. The measured impedance data was divided into two sets, one for developing the model (the "training" data set) and a second for testing the model (the "testing" data set). Fig. 10 shows the membership functions for the three inputs, namely |Z| at 10Hz, phase angle at 10Hz, and battery temperature.

Fig. 11 shows the model-generated data and the "training" data used to develop the model. The average error of the training data using the single frequency impedance measurements is less than 5%! Fig. 12 shows the model-generated data and the "testing" data at 20°C. In the case of the testing data the average testing error is seen to be about twice the error in the model fit to the training data. Nevertheless, the maximum error in the testing data at any of the four temperatures did not exceed 7.5% (although individual data points were in error by as much as 12%.) This is a very good result considering the simplicity of the model.

A more accurate model is presently under development using two different frequency inputs and is expected to

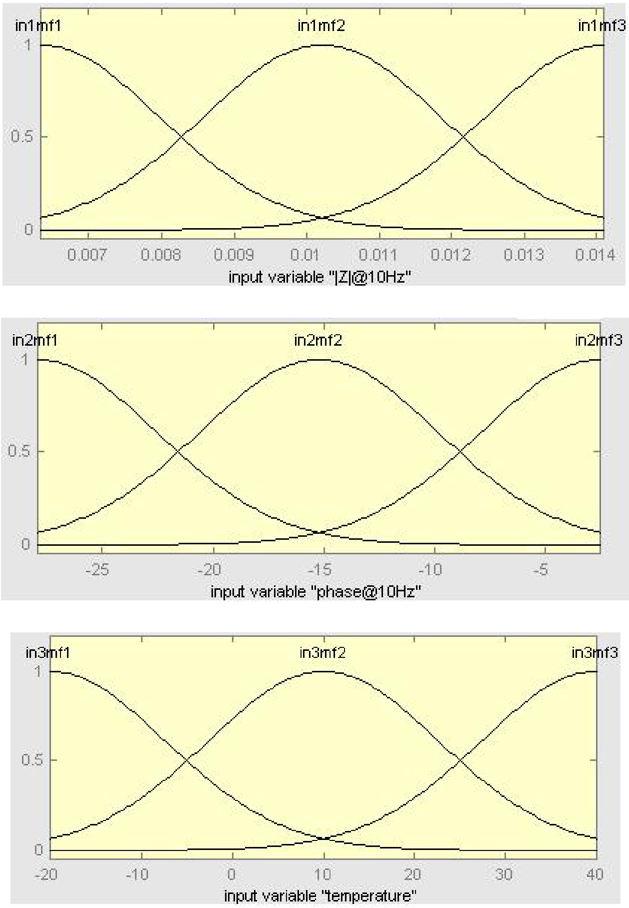

Figure 10. Membership Functions for the three inputs to the SOC estimation fuzzy logic model

yield less than 5% average error with the testing data over the complete temperature range.

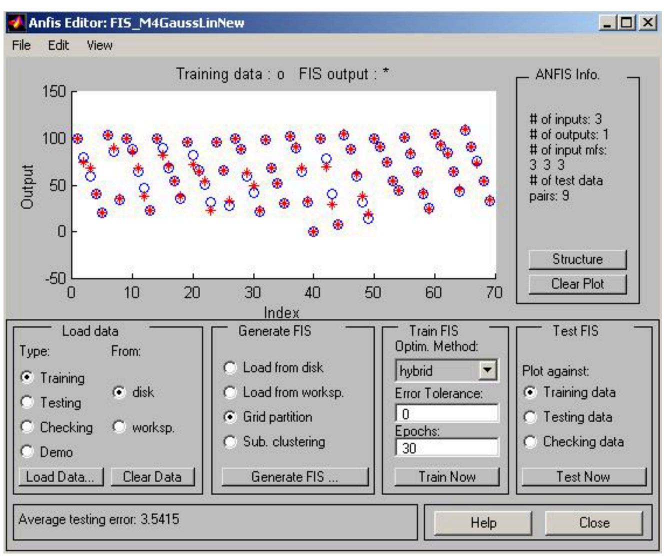

Figure 11. Training data(○) and fuzzy logic model-generated data (*) for SOC estimation of Exide US6TMF batteries at different temperatures over the range -20°C to 40°C

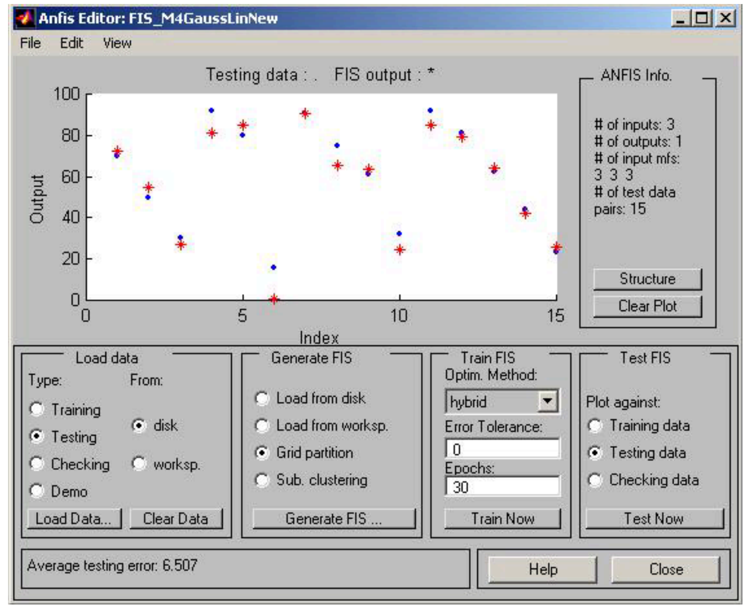

Figure 12. Testing data (●) and fuzzy logic model-generated data (*) for SOC estimation of Exide US6TMF batteries at 20°C

SECOND GENERATION DEVICE

In order to increase the accuracy of the smart battery controller and reduce the size of the smart battery controller and the power consumption further, an improved design is employed in a second-generation unit. A commercial microcontroller, the Motorola 68HC12 with a CAN network interface is used in this second-generation design. This commercial chip contains almost all the required digital functions and the A/D converter. This will save board space. Additionally, the amplified AC signal will not be converted to a DC signal again so that the conversion circuit can also be eliminated saving further space on the board. Another important advantage of this approach is that the error for the impedance caused by this AC/DC conversion is removed, improving the accuracy of the measurement. As long as the two amplified AC signals are sampled, the extraction of the ac impedance magnitude and phase angle can be extracted using software code embedded in the microcontroller. The microcontroller will not generate any noise and the only error caused by the microcontroller is the databus length and the A/D conversion. In order to reduce the effect of the A/D conversion and the databus length, the maximum values and minimum values for these two AC signals are looked for at first, and then the time for three crossing points for these two AC signals are looked for again. The main algorithm is shown in Fig. 13.

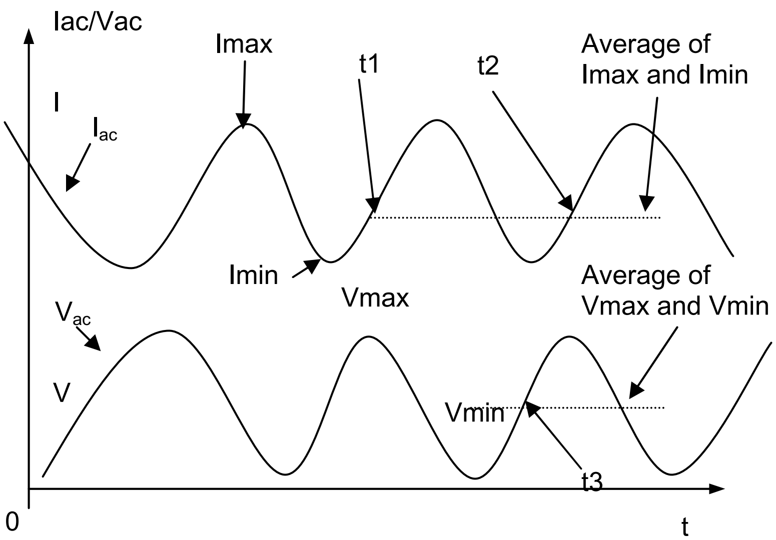

Figure 13. AC Current and Voltage Waveforms entering Microcontroller for Second Generation Design

From Fig. 13, we can easily get Eqs. 1 and 2.

$$\theta = \frac{t3 - t1}{t2 - t1} \cdot 360° \qquad (1)$$

$$/Z/ = \frac{V\max - V\min}{\mathrm{Im}ax - \mathrm{Im}in} \qquad (2)$$

From the theoretical calculations, the accuracy of the impedance measured by this method will be much higher than that by the first generation. Of course, the actual accuracy will also depend on the algorithm employed.

The hardware design for the second-generation unit has been completed and the printed circuit boards fabricated. The software code for extracting the impedance magnitude and phase angle has been written and the received boards have been fabricated and preliminary test results have been obtained. Table 2 shows the magnitude and phase angle for initial testing of the second generation device for a battery at 45% SOC at room temperature.

100Hz		10Hz	
Amplitude	Phase	Amplitude	Phase
5.12 $m\Omega$	-9.12 °	9.21 $m\Omega$	-11.43 °

Table 2. Preliminary test results for second generation smart battery controller.

CONCLUSIONS

In this paper we have presented an embedded smart battery controller for automotive lead acid batteries. We have moved from a previous coulomb counting-based design to one based on ac impedance measurements. Compact, low power, ac impedance measurement circuitry has been presented as well as preliminary test results with this circuitry. We have also presented ac impedance measurements made with a commercial instrument on Exide US 6TMF batteries at different temperatures over the range -20°C to 40°C. From this data we observed sufficient discrimination in the magnitude and phase angles at 10 Hz to suggest that a viable fuzzy logic model to estimate battery SOC was possible. Using these two impedance parameters and the temperature as inputs, we were able to develop a fuzzy logic model to estimate battery SOC to an average accuracy of better than 8%.

A second-generation design which employs a smaller board and uses a Motorola 68HC12 with a CAN network interface has been completed. This second-generation design has been fabricated and initial test results have been presented.

ACKNOWLEDGEMENTS

The authors gratefully acknowledge the support of U.S. Army TACOM (Contract No. DAAE07-01-C-L035) and useful discussions with Dr. Henry Catherino of U.S. Army TACOM, and Fred Feres and Rogan Murdock of Exide Corporation.

REFERENCES

1. P. Singh and C. Fennie, Jr., “A Method for Determining Battery State-of-Charge Using Intelligent Systems,” *U.S. Patent No. 6,011,379* (Jan 4, 2000).
2. C. Fennie, P. Singh, and D.E. Reisner, “A Method for Determining Battery State-of-Health Using Intelligent Systems,” *U.S. Patent No. 6,456,988* (September 24, 2002)
3. H. Chen, P. Singh, X. Wang, and D. Reisner, “Fuzzy Logic-Based Smart Battery SOC Monitor for SLI Batts.,” *Procs. 40th Power Sources Conf.,* Cherry Hill, NJ, Jun 10-13, 2002 pp. 459-462
4. P. Singh, Y.S. Damodar, C. Fennie, and D.E. Reisner, “Fuzzy Logic-Based Determination of Lead Acid Battery State-of-Charge by Impedance Interrogation Methods”, *Procs. EVS-17*, Montreal, Canada, Oct 15-18, 2000
5. The Mathworks, Inc. www.mathworks.com

AUTHOR CONTACT INFORMATION

Chakradhar Pulamarasetty
Dept of Electrical & Computer Engineering

Villanova University
Villanova, PA – 19085.

Dr. Pritpal Singh
Associate Professor
T – 406, Tolentine Hall
Dept of Electrical & Computer Engineering
Villanova University
Villanova, PA – 19085.
singh@ece.vill.edu
Xiquan Wang, Dr. Huiming Chen and Dr. David Reisner
US Nanocorp, Inc.
74 Batterson Park Rd.
Farmington, CT 06032
dreisner@usnanocorp.com

Wsewolod Hnatzcuk
US Army TACOM
AMSTA-TR-E
Warren, MI 48397
wsewolod.hnatczuk@us.army.mil